# Antimony orthophosphate glasses with large nonlinear refractive indices, low two-photon absorption coefficients, and ultrafast response

E. L. Falcão-Filho, Cid B. de Araújo, C. A. C. Bosco, G. S. Maciel, L. H. Acioli, M. Nalin, and Y. Messaddeq

Citation: Journal of Applied Physics **97**, 013505 (2005); doi: 10.1063/1.1828216
View online: http://dx.doi.org/10.1063/1.1828216
View Table of Contents: http://scitation.aip.org/content/aip/journal/jap/97/1?ver=pdfcov
Published by the AIP Publishing

# Antimony orthophosphate glasses with large nonlinear refractive indices, low two-photon absorption coefficients, and ultrafast response

E. L. Falcão-Filho,[a] Cid B. de Araújo, C. A. C. Bosco, G. S. Maciel, and L. H. Acioli
*Departamento de Física, Universidade Federal de Pernambuco, 50670-901 Recife, PE, Brazil*

M. Nalin and Y. Messaddeq
*Instituto de Química, Universidade Estadual Paulista-UNESP, 14800-900 Araraquara, SP, Brazil*

(Received 1 September 2004; accepted 8 October 2004; published online 7 December 2004)

Antimony glasses based on the composition $Sb_2O_3-SbPO_4$ were prepared and characterized. The samples present high refractive index, good transmission from 380 to 2000 nm, and high thermal stability. The nonlinear refractive index, $n_2$, of the samples was studied using the optical Kerr shutter technique at 800 nm. The third-order correlation signals between pump and probe pulses indicate ultrafast response ($<100$ fs) for all compositions. Enhancement of $n_2$ was observed by adding lead oxide to the $Sb_2O_3-SbPO_4$ composition. Large values of $n_2 \approx 10^{-14}$ cm$^2$/W and negligible two-photon absorption coefficients (smaller than 0.01 cm/GW) were determined for all samples. The glass compositions studied present appropriate figure-of-merit for all-optical switching applications. © *2005 American Institute of Physics*. [DOI: 10.1063/1.1828216]

## I. INTRODUCTION

Presently there is an intense search of new materials with improved characteristics for optical applications. In general, photonic materials have to be transparent over large spectral ranges, present high damage threshold to light irradiation and samples of good optical quality have to be easily produced. More specifically, for ultrafast all-optical switching or optical signal processing, the required characteristics of materials are well established. The materials have to present large nonlinear (NL) refractive index, $n_2$, small linear absorption coefficient, $\alpha_0$, low two-photon absorption coefficient, $\alpha_2$, and dynamic response in the sub-picosecond range. Of course, low absorption coefficients can be observed for optical wavelengths far from resonance but in contrast the NL response is enhanced near resonance. Thus, the selection of a material suitable to present good performance for particular applications requires a careful investigation.

One possible approach to obtain highly NL materials is the development of glasses with a large proportion of hyperpolarizable entities presenting low absorption in selected spectral range. Indeed, glasses with heavy metal ions and vitreous ceramics containing dielectric or metallic nanoparticles have been considered for various specific uses.[1–8]

Among the available NL materials antimony glasses (AG) are emerging as promising systems for photonic applications. In the past, the research on $Sb_2O_3$-based glasses was dedicated mainly to the glass formation and their thermal properties.[9–13] Glass transition temperature of $\approx$300 °C, refractive index of $\approx$2, good infrared transmittance and high thermal stability are some characteristics presented by these glasses. Recently new methods of preparation have been developed and samples having improved optical quality can be obtained.[14,15] NL optics experiments in antimony and lead oxyhalide glasses, performed at 532 nm, have shown large NL absorption coefficients up to 20 cm/GW that indicate the possible use of these glasses for optical limiting.[16] Photoinduced structural changes in amorphous films of antimony-polyphosphate were observed in samples submitted to ultraviolet irradiation.[17] More recently, the nonlinearity of antimony-polyphosphate glasses (APPG) was characterized in the femtosecond regime at 800 nm. Large NL refractive index, $n_2$, was obtained and increase of $n_2$ by $\approx$80% was observed adding lead oxide in the glass composition.[18] Although APPG are not hygroscopic, the hygroscopy of the starting compound $Sb(PO_3)_3$ contributes to narrow the glass domain that varies from 15 to 35 molar percent of $Sb(PO_3)_3$. Also a residual amount of water is observed in its structure by infrared absorption.[15,19] In general, the large nonlinearity of AG is mainly attributed to the high polarizability of $Sb^{3+}$ but appropriate chemical elements added to the AG composition may contribute to increase their nonlinearity.

In this paper we present a study of the NL optical properties of antimony-orthophosphate glasses. This new glass composition does not present residual water and has a glass domain that varies from 7.5 to 75 molar percent of antimony-orthophosphate ($SbPO_4$) with large thermal stability.[15,19] The NL measurements were performed on the binary system $Sb_2O_3-SbPO_4$ and the ternary composition $Sb_2O_3-SbPO_4-PbO$. In Sec. II it is described the method of samples preparation and the techniques used for their characterization. The NL optical properties of the samples, probed in the near-infrared (800 nm) with laser pulses of 100 fs, are presented in Sec. III. Values of $n_2$ corresponding to various compositions were measured and a classical model was used to estimate $n_2$ for comparison with the experimental results. Also the possible use of the glasses studied for all-optical switching is evaluated. In Sec. IV it is presented a summary of the main conclusions.

[a]Author to whom correspondence should be addressed. Electronic mail: elff@df.ufpe.br

 

TABLE I. Samples studied and characteristic temperatures ($T_g$ is the glass transition temperature and $T_x$ is the onset of crystallization).

| Group | Sample | Composition (% mol) | $T_g$ (°C) | $T_x$ (°C) | $T_x - T_g$ (°C) |
|---|---|---|---|---|---|
| 1 | A | $70Sb_2O_3-30SbPO_4$ | 294 | 372 | 78 |
| | B | $60Sb_2O_3-40SbPO_4$ | 317 | 423 | 106 |
| | C | $50Sb_2O_3-50SbPO_4$ | 318 | 410 | 92 |
| | D | $40Sb_2O_3-60SbPO_4$ | 325 | 400 | 75 |
| 2 | E | $50Sb_2O_3-40SbPO_4-10PbO$ | 316 | 406 | 90 |
| | F | $30Sb_2O_3-50SbPO_4-20PbO$ | 334 | 445 | 111 |

## II. EXPERIMENTAL DETAILS

Synthesis of the samples was carried out by melting starting materials ($Sb_2O_3$ grade purity 99% and $SbPO_4$ prepared according to Refs. 15 and 19) inside glassy carbon crucibles in an electrical furnace for 10 min at 700–900 °C in air. For less stable glasses, the liquid melt was quenched between two brass pieces, from which samples with thickness of 3 mm or less were prepared. Sample thicknesses up to 10 mm could be obtained for compositions less prone to devitrification by casting the liquid into a brass mold at a temperature around 250 °C. Large samples were annealed around the glass transition temperature for 2 hours to reduce thermal stress.

Glass transition temperatures and the onset of crystallization temperatures were determined by differential scanning calorimetry. For these measurements powdered samples were heated at a rate of 10 K/min within aluminum pans in $N_2$ atmosphere. The structural organization of the glass samples has been studied by far-infrared absorption (FTIR), Raman scattering, nuclear magnetic resonance, Mössbauer spectroscopy, extended x-ray absorption fine structure (EXAFS) and x-ray absorption near edge structure (XANES) at K and $L_{3,1}$–Sb edges.[19,20] The combination of the new method of preparation and its improvement based on the characterization of the glasses by various techniques allowed to obtain samples of good optical quality in a controlled manner. More details on the samples preparation are presented in Ref. 19. Samples with dimensions of $15\times15\times2$ mm$^3$ were cut and polished for the optical measurements.

The absorption spectra from 200 to 2000 nm were obtained using a double beam spectrophotometer, and the linear index of refraction was measured at 632.8 nm and at 1550 nm using the prism-coupler technique. For these measurements the samples with optically polished surfaces were faced on a prism mounted on a rotary table. The light beam from a He–Ne or from a diode laser was sent to the base of the prism and reflection is measured by a photodetector. The signal from the photodetector, plotted for different angles of incidence of the beam, allows to determine the intensity coupled to the sample, and from this experiment the refractive index is calculated.

The light source used in the nonlinear experiments at 800 nm was a laser system consisting of CW Nd: YAG laser pumping a Ti: Sapphire crystal. The laser system delivers ≈100 fs pulses at a repetition rate of 82 MHz. A Kerr shutter setup[21] with homodyne detection was employed to characterize the NL response of the samples.

## III. RESULTS AND DISCUSSION

Two glass groups with different compositions were studied as presented in Table I. In the first group, a binary composition of $Sb_2O_3-SbPO_4$, with various relative concentrations of $Sb_2O_3$ and $SbPO_4$ was investigated. The second group was obtained adding lead oxide (PbO) to the composition of the first group. The glass transition temperature, $T_g$, the onset of crystallization, $T_x$, and the thermal stability range, $T_x-T_g$, are also indicated in Table I.

Figure 1 shows the results of the linear optics experiments performed. The optical absorption spectra of all samples are presented in Figs. 1(a) and 1(b) while the refractive indices, $n_0$, are shown in Fig. 1(c). The samples present large transmission window from ≈380 to ≈2000 nm. High refractive indices from 1.87 to 2.03 were measured and their high values give a good indication that the samples are highly NL, according to the Miller's rule.[21] It is clear in Fig. 1 that $n_0$ increases due to the presence of PbO in the samples of Group 2.

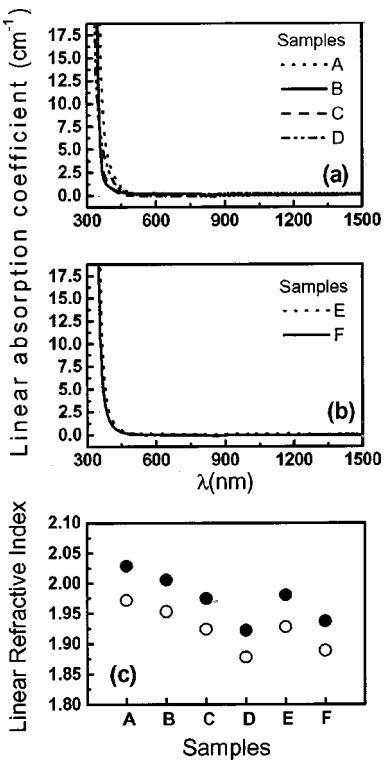


FIG. 1. (a), (b) Linear absorption coefficient as a function of wavelength. (c) Refractive index of samples. Measurements at 633 nm (●) and at 1550 nm (○).

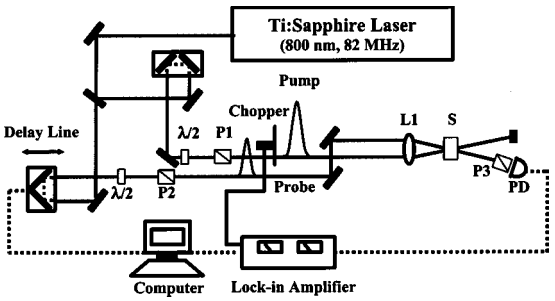


FIG. 2. Schematic of the experimental setup. $\lambda/2$ represents the half-wave plates. P1–P3 stand for Glan prisms. L1 is a lens and *S* is the sample.

The NL refractive indices and the temporal response of the nonlinearity were investigated using a Kerr shutter setup. A scheme of the experimental system is shown in Fig. 2. The light beam from the Ti:Sapphire laser was split into two linearly polarized beams with 1:10 intensity ratio which are overlapped on the sample. The crossing angle between the beams is ~6° and the sample was placed between crossed oriented polarizers. The stronger (pump) beam induces a refractive index change in the sample, $\Delta n(t)=n_2 I_{\text{pump}}(t)$, where $I_{\text{pump}}(t)$ is the pump beam intensity. The probe beam with its polarization set at 45° with respect to the pump beam polarization is used to investigate the dynamics of $\Delta n(t)$ and its magnitude. The beams were focused by a 10 cm focal length lens, and the intensity of the pump beam at the focus was ~2 GW/cm$^2$. A lock-in amplifier was used in synchronism with a chopper, operated at 400 Hz, placed in the pathway of the probe beam to facilitate the detection.

When the axis of the two polarizers are perpendicular a small fraction of the probe beam intensity leaks out the polarizer-analyzer located in front of the photodiode and this allows for homodyne detection of $\Delta n(t)$. During the presence of the pump beam, the probe beam polarization is rotated due to the birefringence induced by the pump beam with a dynamical behavior that depends on the material response time and the laser pulse duration. Consequently a larger fraction of the probe beam intensity reaches the photodiode. The lock-in amplifier provides a temporally averaged signal $S(\tau) \propto \langle \Delta n(t) \times I_{\text{probe}}(t+\tau) \rangle$ for each delay time, $\tau$, between pump and probe pulses spatially overlapped at the sample position. The signal $S(\tau)$ was monitored by scanning a delay-line that allowed for different values of $\tau$. $S(\tau) \neq 0$ when the laser pulses are temporally overlapping and is null when $\tau$ is larger than the pulse duration.

To illustrate the sensitivity of the experimental setup we show in Fig. 3(a) the correlation signal $S(\tau)$ for a 3.2 mm-thick slab of fused quartz. Figures 3(b) and 3(c) show the behavior of $S(\tau)$ for samples with the different compositions presented in Table I. All samples present larger nonlinearities than fused quartz. For the assumed hyperbolic secant pulse shape, the symmetric correlation signal of width equal to 155 fs implies that the samples have a response faster than ≈100 fs. This means that the origin of the nonlinearity may be attributed to electronic processes either alone or in combination with other processes whose characteristic times are shorter than 100 fs.

It was observed that the symmetrical shape of $S(\tau)$ as a function of $\tau$ does not change for increasing laser power while its amplitude increases. A linear dependence of the signal amplitude versus the pump laser power was measured, as expected for a homodyne Kerr shutter signal, and this behavior indicates that no saturation effect is taking place. Also, variation of the samples' transmittance as a function of the pump beam intensity was not observed in all experiments at 800 nm, which implies that the two-photon absorption coefficient of all samples is below our detection limit ($\alpha_2 < 0.01$ cm/GW).

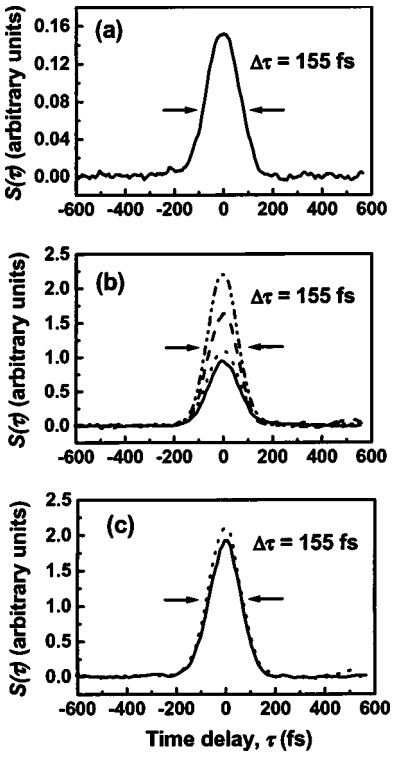


FIG. 3. Temporal evolution of the Kerr shutter correlation signal vs the delay time between pump and probe laser pulses. (a) Reference sample (fused quartz). (b) Samples of Group 1: A (dash–dot–dot line); B (dotted line); C (solid line); D (dashed line). (c) Samples of Group 2 E (dotted line); F (solid line).

The magnitude of $n_2$ is obtained by comparison with the nonlinear refractive index of fused quartz, $2.2 \times 10^{-16}$ cm$^2$/W,[22] which was used as a calibration standard. The experimental values of $n_2$ are given in Table II for all samples. The data show that the binary composition presenting the largest NL refractive index (sample A) has nonlinearity ≈50 times larger than fused quartz. Another important

TABLE II. Nonlinear refractive index. Experimental values, $n_2$, and theoretical values, $n_2^{\text{theo}}$ and $\tilde{n}_2$. $\upsilon_d$ is the Abbe number.

| Sample | $n_2^{\text{exp}}$ ($10^{-14}$ cm$^2$/W) | $n_2^{\text{theo}}$ ($10^{-14}$ cm$^2$/W) | $\upsilon_d$ | $\tilde{n}_2$ ($10^{-14}$ cm$^2$/W) |
|---|---|---|---|---|
| A | 1.0±0.2 | 1.0 | 17.90 | 1.2 |
| B | 0.6±0.1 | 0.9 | 19.08 | 1.0 |
| C | 0.5±0.1 | 0.8 | 19.17 | 1.0 |
| D | 0.8±0.1 | 0.7 | 20.79 | 0.8 |
| E | 1.1±0.2 | 0.9 | 18.35 | 1.1 |
| F | 1.0±0.2 | 0.8 | 19.55 | 0.9 |

point is that sample E which contains 10% of lead oxide has ≈100% larger nonlinearity than sample B, C, and D. Sample F also presents enhanced nonlinearity with respect to samples B, C, and D due to the presence of PbO in its composition. The enhancement of the $n_2$ value is attributed to $Pb^{2+}$ that has larger polarizability than $Sb^{3+}$. Also we recall that the structural analysis of the binary samples revealed the existence of two types of structure in the glass. For $Sb_2O_3$ concentration larger than 50% the structure of antimony-oxide is dominant. Below 50% the structure of antimony-phosphate becomes dominant. The change of local structure may be correlated with the increase of $n_2$ in sample D.

Using a model based on a classical nonlinear oscillator [Boiling, Glass, and Owyoung (BGO) model],[23] it was possible to estimate values for $n_2$ which are in agreement with the experimental data. In the BGO-model the third-order polarizability is assumed to be proportional to the linear polarizability squared and the optical dispersion of the medium is determined by a single resonance at $\hbar\omega_0$. The incident light field of frequency $\omega$ is supposed to be far from resonance ($\omega \ll \omega_0$) and the NL refractive index, written in Gaussian units, is given by

$$n_2[esu] = \frac{(n_0(\lambda)^2+2)^2(n_0(\lambda)^2-1)^2}{48\pi n_0(\lambda)\hbar\omega_0} \times \frac{(gs)}{(Ns)}, \tag{1}$$

where $c$ is the speed of light in m/s, $N$ is the density of nonlinear oscillators, $s$ is the effective oscillator strength, $g$ is a dimensionless parameter given by $g=\mu s\hbar/m\omega_0$, where $\mu$ is the nonlinear coupling coefficient, $(2\pi\hbar)$ is the Planck's constant, and $m$ is the electron mass. The linear refractive index for light wavelength $\lambda$ is denoted by $n_0(\lambda)$ and, according to Ref. 23, satisfies the expression

$$\frac{4\pi}{3}\frac{(n_0(\lambda)^2+2)}{(n_0(\lambda)^2-1)} = \frac{\omega_0^2-\omega^2}{(e^2/m)(Ns)}, \tag{2}$$

where $e$ is the electron charge in Gaussian units.

The parameters $Ns$ and $\omega_0$ in Eq. (2) can be obtained from the values of $n_0(\lambda=633\ \text{nm})$ and $n_0(\lambda=1550\ \text{nm})$ given in Fig. 1 for each sample. Then, the values obtained for $Ns$ and $\omega_0$ are introduced in Eq. (1) to determine $n_2$. The parameter $gs$ was shown in Ref. 24 to be material dependent and changes with the magnitude of the nonlinearity. The value of $gs$ was estimated considering $s=3$ because it is an appropriate value for oxides[23] and it is in good agreement with the estimated values for our samples as obtained by the ratio $Ns/N_{ox}$, where $N_{ox}$ is the oxygen ions density. Since our samples have energy gap ≈50% smaller than the materials investigated in Ref. 23 for which $g=1$, and considering that $g \propto 1/\omega_0$, it is reasonable to assume $g=2$ for our samples. Thus, we obtain $gs=6$ which is in agreement with the results determined through the best fitting of the data. The value of $n_0(\lambda=800\ \text{nm})$ considered in Eq. (1), was calculated using Eq. (2) with the values of $Ns$ and $\omega_0$ obtained for each sample. The results obtained for $n_2$ at 800 nm are shown in Table II for comparison with the experimental values. In order to allow direct comparison with most papers we present the results in units of $[\text{cm}^2/\text{W}]$ obtained through the relation $\{40\pi/10^4\ cn_0(\lambda)\}n_2[esu]$.

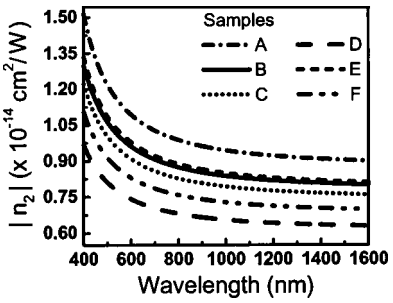


FIG. 4. Chromatic dispersion of the nonlinear refractive index (prediction based on the BGO-model).

Equations (1) and (2) were also extended to predict the spectral behavior of $n_0$ and $n_2$ in the visible and in the near-infrared range. The results for $n_2$ are presented in Fig. 4 for all samples where it is observed a small chromatic dispersion in the infrared range. Furthermore, using the spectral dependence of $n_0$, deduced from Eq. (2), it was possible to calculate the Abbe number, $\upsilon_d$, which is related to $n_2$ by

$$\tilde{n}_2(esu) = \frac{136(n_d-1)(n_d{}^2+2)^2}{\upsilon_d\left[1.517+\upsilon_d\dfrac{(n_d-1)(n_d{}^2+2)}{6n_d}\right]^{1/2}}, \tag{3}$$

where $n_d$ is the refractive index at 587.56 nm and $\upsilon_d$ is the Abbe number. The results are given in Table II which includes values for $\upsilon_d$ and $\tilde{n}_2$.

To evaluate the performance of the AG in all-optical switching devices we recall that suitable materials for such application must have $n_2$ values large enough to achieve switching for a sample thickness comparable to the absorption length. Accordingly, a good material for all-optical switching using the NL Fabry–Perot configuration should satisfy $W=\Delta n_{max}/\lambda\alpha_0 > 0.27$,[25] where $\Delta n_{max}$ is the maximum light-induced refractive index change achievable. The figure-of-merit to evaluate the material performance with respect to the two-photon absorption is $T=2\alpha_2\lambda/n_2$ which has to be smaller than 1, irrespective of the device.[25]

Figure 5 shows the results obtained for $W$ and $T$. Calculations of $W$ were done for values of $\Delta n_{max}$ corresponding to the largest intensity employed in the present experiments. On the other hand, the values of $T$ for all samples were calculated considering $\alpha_2=0.01$ cm/GW, although its actual value may be smaller. Such low value of $\alpha_2$ is because twice the laser photon energy is smaller than the energy band gap, $E_g$, of the samples. The results obtained indicate, for all samples compositions, a large potential for photonic applications.

Clearly, it is of interest to extend the present evaluation for the optical wavelength used in the telecommunication networks, around 1.5 $\mu$m. Although NL measurements at the communications wavelengths were not performed, we estimated using the BGO model that $n_2 \approx 0.6-0.9 \times 10^{-14}$ cm$^2$/W at 1.5 $\mu$m. For this wavelength the value of $\alpha_2$ is expected to decrease due to the larger two-photon energy detuning with respect to $E_g$ and consequently the value of $T$ will be smaller than at 800 nm.

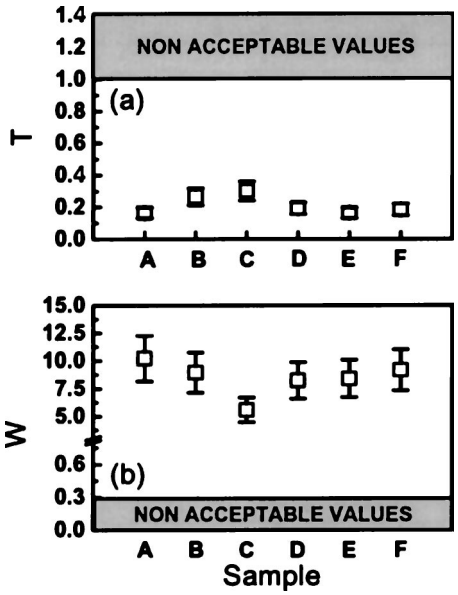


FIG. 5. Figure-of-merit for all-optical switching.

## IV. SUMMARY

The synthesis and the optical characterization of new antimony based glasses for photonic applications were reported. Binary glass samples with composition $Sb_2O_3$–$SbPO_4$, having large nonlinear refractive indices and good figure-of-merit for all-optical switching, were investigated. Also ternary glasses obtained by incorporation of PbO in the binary glasses were studied. Large enhancement of the NL properties was observed due to the introduction of PbO. On the basis of the results presented it is concluded that antimony-orthophosphate glasses can be successfully used for all-optical switching in the sub-picosecond domain.

## ACKNOWLEDGMENTS

We acknowledge the financial support by the Brazilian agencies Conselho Nacional de Desenvolvimento Científico e Tecnológico (CNPq) and Fundação de Amparo à Ciência e Tecnologia do Estado de Pernambuco (FACEPE).

[1]M. Yamane and Y. Asahara, *Glasses for Photonics* (Cambridge University Press, Cambridge, 2000).
[2]U. Woggon, *Optical Properties of Semiconductor Quantum Dots* (Springer, Berlin, 1997).
[3]E. L. Falcão-Filho, C. A. C. Bosco, G. S. Maciel, L. H. Acioli, C. B. de Araújo, A. A. Lipovskii, and D. K. Tagantsev, Phys. Rev. B **69**, 134204 (2004) and references therein.
[4]V. M. Shalaev, *Nonlinear Optics of Random Media* (Springer, Berlin, 2000).
[5]V. A. Shubin, A. K. Sarychev, J. P. Clerc, and V. M. Shalaev, Phys. Rev. B **62**, 11230 (2000).
[6]G. Boudebs, S. Cherukulappurath, M. Guignard, J. Troles, F. Smektala, and F. Sanchez, Opt. Commun. **232**, 417 (2004).
[7]I. Kang, S. Smolorz, T. Krauss, F. Wise, B. G. Aitken, and N. F. Borrelli, Phys. Rev. B **54**, R12641 (1996).
[8]S. Smolorz, I. Kang, F. Wise, B. G. Aitken, and N. F. Borrelli, J. Non-Cryst. Solids **256&257**, 310 (1999).
[9]B. Dubois, H. Aomi, J. J. Videau, J. Portier, and P. Haggenmuller, Mater. Res. Bull. **19**, 1317 (1984).
[10]B. Dubois, J. J. Videau, M. Couzi, and J. Portier, J. Non-Cryst. Solids **88**, 355 (1986).
[11]M. M. Ahmed and D. Holland, Glass Technol. **28**, 141 (1987).
[12]W. H. Dumbaugh and J. C. Lapp, J. Am. Chem. Soc. **75**, 2315 (1992).
[13]A. Datta, A. K. Giri, and D. Chakravorty, Phys. Rev. B **47**, 16242 (1993).
[14]G. Poirier, M. Poulain, and M. Poulain, J. Non-Cryst. Solids **284**, 117 (2001).
[15]M. Nalin, M. Poulain, M. Poulain, S. J. L. Ribeiro, and Y. Messaddeq, J. Non-Cryst. Solids **284**, 110 (2001).
[16]R. E. de Araujo, C. B. de Araújo, G. Poirier, M. Poulain, and Y. Messaddeq, Appl. Phys. Lett. **81**, 4694 (2002).
[17]F. S. de Vicente, M. S. Li, M. Nalin, and Y. Messaddeq, J. Non-Cryst. Solids **330**, 168 (2003).
[18]E. L. Flacão-Filho, C. A. C. Bosco, G. S. Maciel, C. B. de Araújo, L. H. Acioli, M. Nalin, and Y. Messaddeq, Appl. Phys. Lett. **83**, 1292 (2003).
[19]M. Nalin, Doctor Thesis, Instiuto de Química—Araraquara, Universidade Estadual Paulista, 2002.
[20]M. Nalin, Y. Messaddeq, S. J. L. Ribeiro, M. Poulain, G. Brunklaus, C. Rosenhahn, B. D. Mosel, and H. Eckert, J. Mater. Chem. (to be published).
[21]Y. R. Shen, *The Principles of Nonlinear Optics* (Wiley, New York, 1984).
[22]R. De Salvo, A. A. Said, D. J. Hagan, E. W. Van Stryland, and M. Sheik-Bahae, IEEE J. Quantum Electron. **32**, 13 (1996).
[23]N. L. Boiling, A. J. Glass, and A. Owyoung, IEEE J. Quantum Electron. **14**, 601 (1978).
[24]I. Kang, T. D. Krauss, F. W. Wise, B. G. Aitken, and N. F. Borrelli, J. Opt. Soc. Am. B **12**, 2053 (1995).
[25]G. I. Stegeman, in *Nonlinear Optics of Organic Molecules and Polymers*, edited by H. S. Nalva and S. Miyata (CRC, Boca Raton, Fl., 1997), p. 799.